

Electronic Supplementary Information

A Novel Crystalline Azine-Linked Three-Dimensional Covalent Organic Framework for CO₂ Capture and Conversion

Pengxin Guan^a, Jikuan Qiu^a, Yuling Zhao^a, Huiyong Wang^{a*}, Zhiyong Li^a,
Yunlei Shi^b and Jianji Wang^{a*}

^a Collaborative Innovation Center of Henan Province for Green Manufacturing of Fine Chemicals, Key Laboratory of Green Chemical Media and Reactions, Ministry of Education, School of Chemistry and Chemical Engineering, Henan Normal University, Xinxiang, Henan 453007, P. R. China

^b College of Chemistry and Chemical Engineering, Lanzhou University, Lanzhou, Gansu 730000 (P. R. China)

*E-mail: jwang@htu.cn; hywang@htu.cn

Table of Contents

Section S1. Materials and Methods (pages S2-S4)

Section S2. Figures S1-16 (pages S5-S10)

Section S3. Tables S1-7 (pages S10-S14)

Section S4. References (page S14)

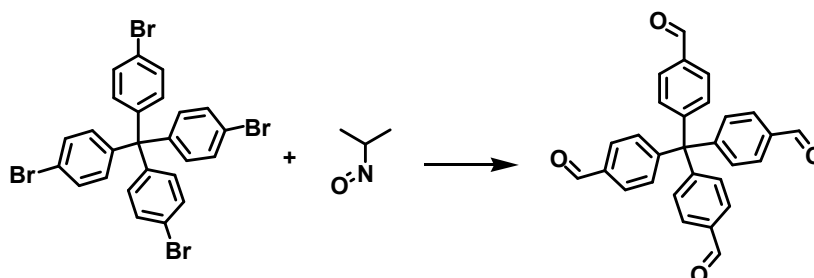
Section S1: Materials and Methods

All chemicals and reagents were commercially available and used without further purification. Ionic liquid [Bmim][Tf₂N] were synthesized according to the published procedures ^[1,2]. Fourier transform infrared (FTIR) spectra of the samples were collected on a Spectrum 400 spectrometer (Perkin-Elmer). Power X-ray diffraction (PXRD) data were obtained with a Bruker D₈ Advance diffractometer at 40 kV and 40 mA with Cu K radiation from $2\theta = 2^\circ$ to 40° in 0.05° increment. Thermal properties of the materials were evaluated using a thermogravimetric analysis (TGA) instrument (STA449C) over the temperature range from 25 °C to 800 °C under N₂ atmosphere with a heating rate of 10 °C/min. ¹H NMR and ¹³C NMR spectra were recorded on a Bruker AVANCE III HD 600 spectrometer where deuterated solvents (DMSO-d₆, and CDCl₃) were used. Solid-state NMR experiments were performed on an AVANCE III HD 500 MHz spectrometer.

Nitrogen adsorption and desorption isotherms were measured at 77 K using a Micromeritics ASAP 2010 system. The samples were treated at 120 °C for 8 h before measurements. Specific surface areas were calculated from the adsorption data using Langmuir and Brunauer-Emmett-Teller (BET) methods. Pore size distribution data were calculated based on the nonlocal density functional theory (NLDFT) model in the Micromeritics ASAP2010 software package. Field emission scanning electron microscopy (SEM) observations were performed on a Hitachi SU8010 microscope operated at an accelerating voltage of 10.0 kV. Transmission electron microscopy (TEM) images were obtained with a JEOL-JEM-2010 transmission electron

microscope operated at 200 kV.

1.1 General procedures for the synthesis of tetrakis(4-formylphenyl)methane (TFPM)^[2]



A mixture of tetrakis(4-bromophenyl)methane (1.0 g, 1.57 mmol) in THF (75 mL) was placed in a dry 250 mL round bottom flask. The solution was cooled down to -78 °C under N₂. Then a solution of n-butyllithium (1.6 M in hexane, 14.3 mmol) was added dropwise. The mixture was kept for 30 min at -78 °C and then anhydrous dimethylformamide (2.3 mL, 28.5 mmol) was added. The resulting green suspension was allowed to warm up to room temperature overnight. After the reaction was completed, the solution was treated with 1 M HCl, extracted with ethyl acetate, and dried under vacuum. The solvent was evaporated, and the crude yellow product was further purified by chromatography via a column using silica gel.

1.2 Synthetic Procedures for 3D-HNU5 in [Bmim][Tf₂N]

0.036 mmol of tetrakis(4-formylphenyl)methane (TFPM) was dissolved in [Bmim][Tf₂N] (3uL) with vigorous stirring. Then, 0.074 mmol (3.71 mg) of NH₂NH₂·H₂O was added in the mixture and stirred at room temperature for 12 h. The precipitate was isolated by filtration and washed with acetone (30 mL) and ethanol (30 mL) separately. The collected powder was then activated by solvent exchange with anhydrous methanol for 3 times and dried at 120 °C under vacuum for 12 h to

give a light yellow colored powder with up to 81% isolated yield.

1.3 CO₂ Absorption

Low-pressure CO₂ (<1 bar) absorption measurements were performed using a Micromeritics ASAP 2010 system. Before the measurements, about 0.1 g samples were loaded into the sample tube and then degassed under dynamic vacuum at 150 °C for 8 h. CO₂ absorption isotherms were measured at 273 K.

1.4 Synthesis of 3D-HNU5@Ag^[3]

In a 100 mL round-bottom flask, AgBF₄ (5.0 mg) was dissolved in 20 mL of THF, and then 3D-HNU5 (100 mg) was added under nitrogen. The mixture was kept stirring for 24 h at 80 °C in dark. Finally, the resulting solid was isolated by filtration and washed with THF, and then purified using Soxhlet extraction (THF) for 24 h. The 3D-HNU5@Ag was obtained after drying at 100 °C under vacuum for 12 h.

1.5 Typical procedures for the cycloaddition of propargylic alcohols with CO₂

In a 10 mL Schlenk flask, propargylic alcohols (1.0 mmol), DBU (1.0 mmol), CH₃CN (3 mL) and indicated amount of the catalyst were added. The flask was capped with a stopper and then sealed. The gas-exchanging process was conducted using “freeze–pump–thaw” method. The reaction mixture was stirred at 25 °C for 12 h under CO₂ atmosphere (balloon). After the reaction was finished, 5 mL water was added in the mixture, and the products were extracted with EtOAc to obtain the desired carbonates.

Section S2: Figures

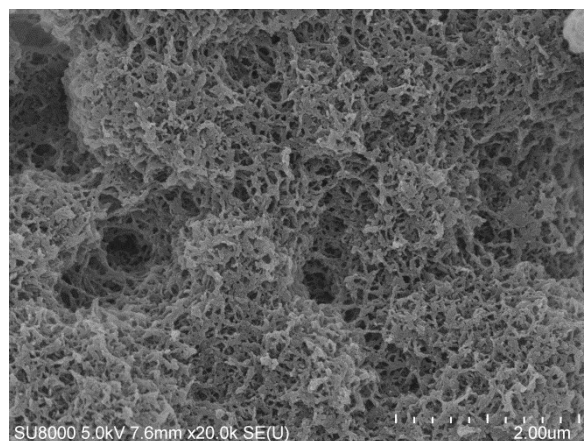


Figure S1. SEM images of the 3D-HNU5.

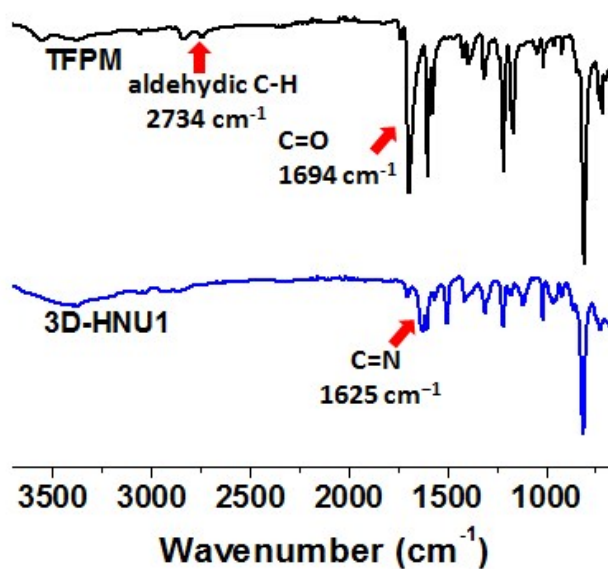


Figure S2. FT-IR spectra of TFPM (black) and the as-synthesized 3D-HNU5 (blue).

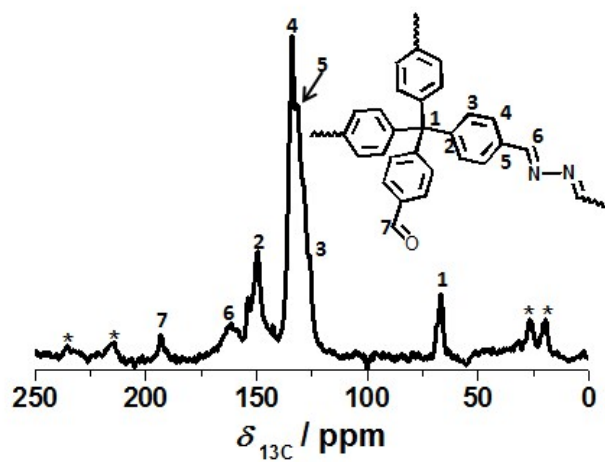


Figure S3. ^{13}C CP-MAS NMR spectra and carbon signal assignment of 3D-HNU5, the asterisks denote the spinning sidebands.

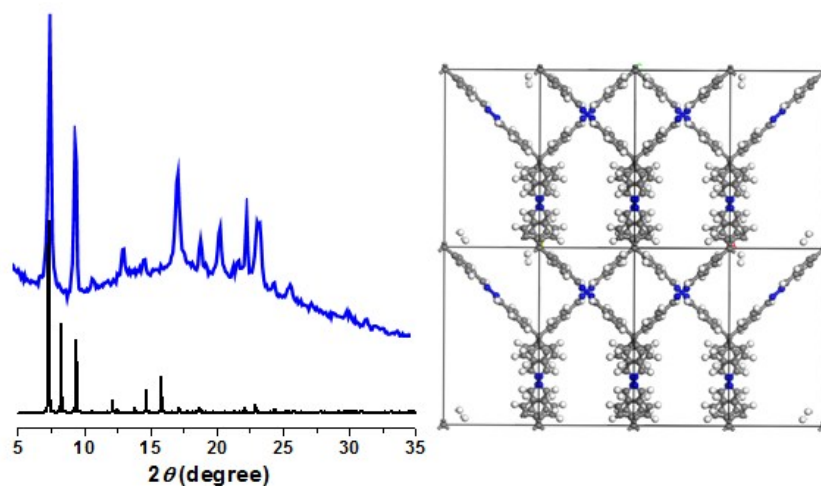


Figure S4. Calculated PXRD pattern of the 3D-HNU5 based on the 2-fold interpenetrated diamond net.

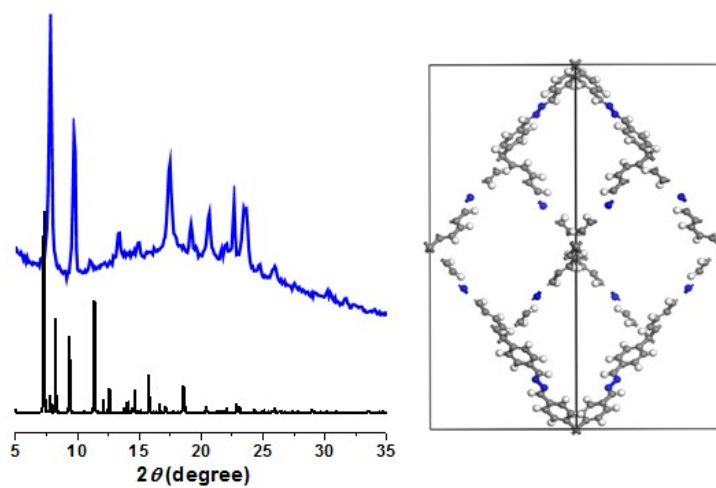


Figure S5. Calculated PXRD pattern of the 3D-HNU5 based on the non-interpenetrated diamond net.

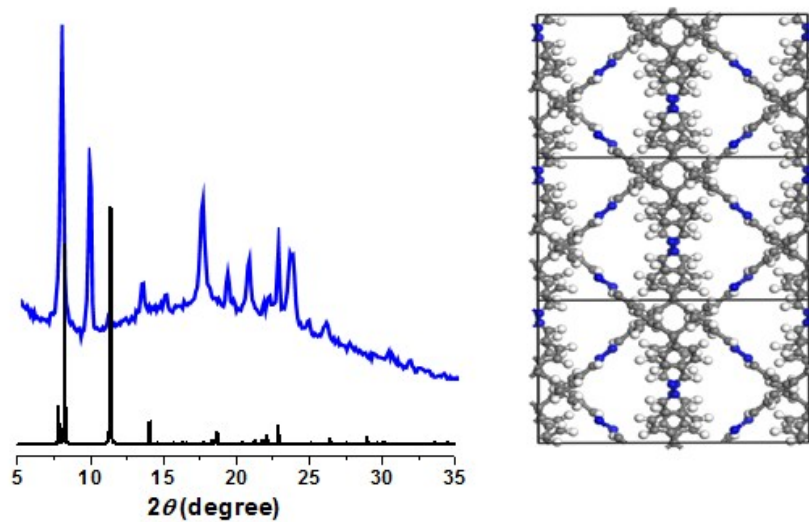


Figure S6. Calculated PXRD pattern of the 3D-HNU5 based on the 3-fold interpenetrated diamond net.

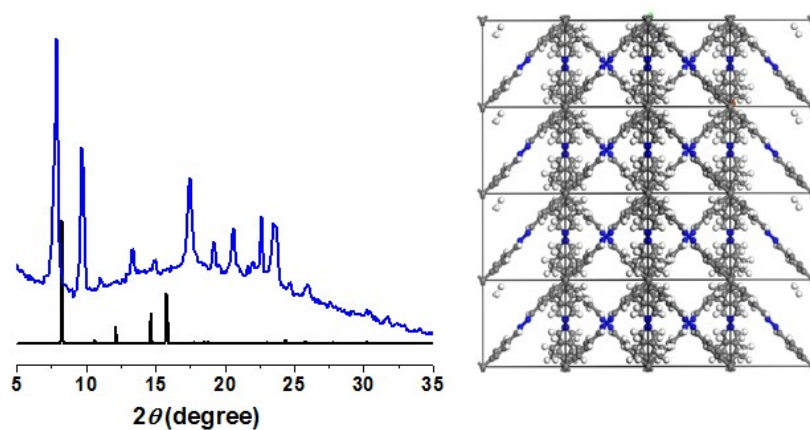


Figure S7. Calculated PXRD pattern of the 3D-HNU5 based on the 4-fold interpenetrated diamond net.

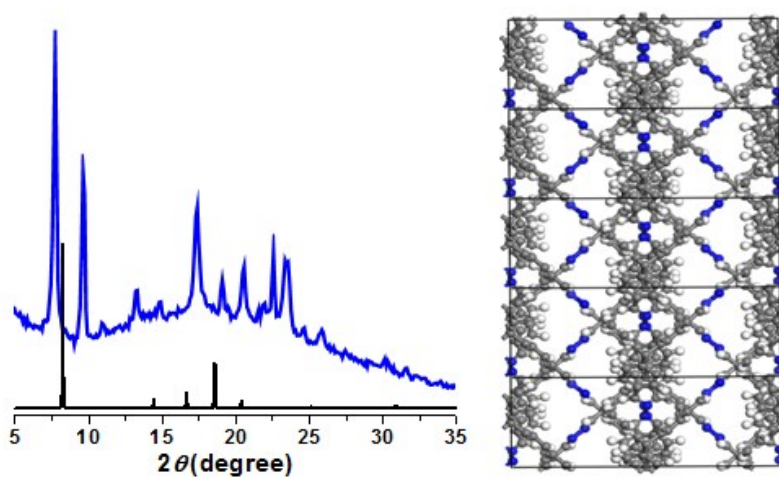


Figure S8. Calculated PXRD pattern of the 3D-HNU5 based on the 5-fold interpenetrated diamond net.

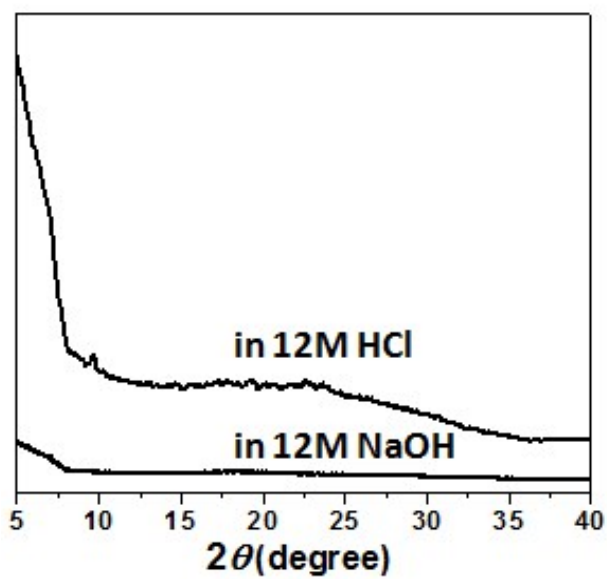


Figure S9. PXRD patterns of 3D-HNU5 treated with 12M HCl and 12M NaOH for 48 h.

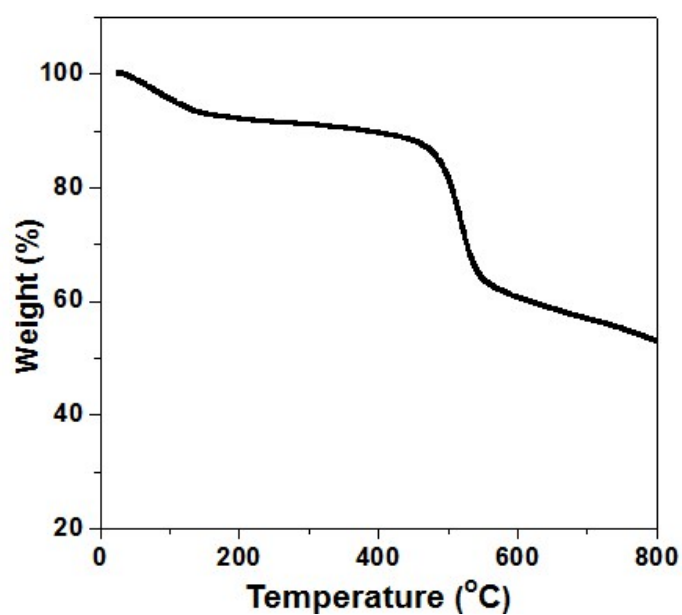


Figure S10. TGA curve of the as-synthesized 3D-HNU5 under N_2 atmosphere and showing the high thermal stability.

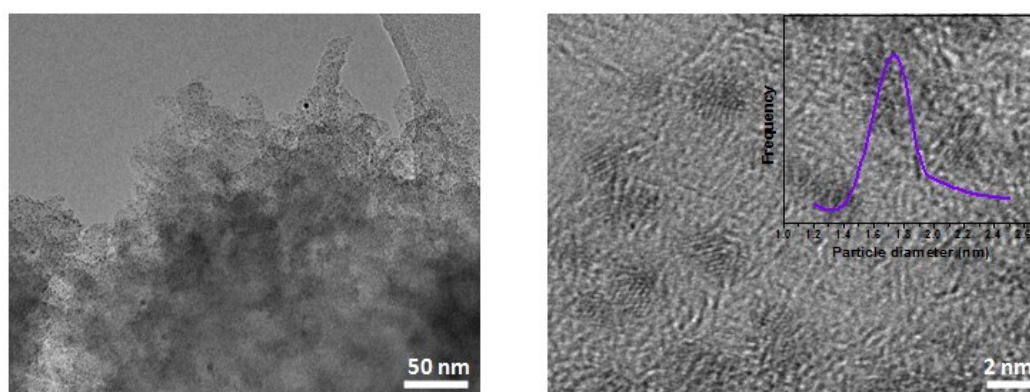


Figure S11. High-resolution TEM images of the Ag@3D-HNU5.

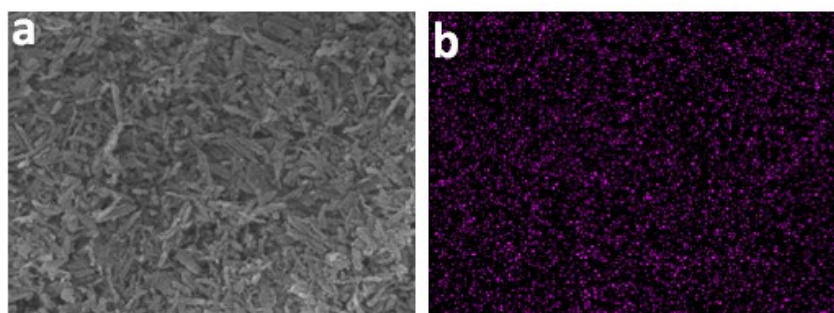


Figure S12. Element maps for Ag@3D-HNU5 sample: left, SEM image; right, EDS image of Ag (purple).

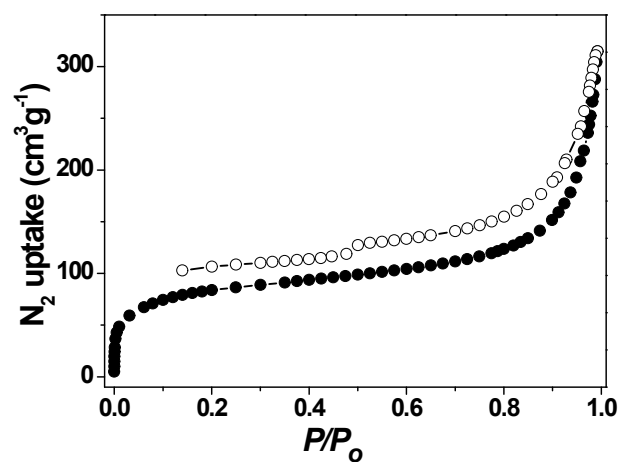


Figure S13. N₂ adsorption-desorption isotherms of Ag@3D-HNU5: adsorption, filled symbols; desorption, empty symbols.

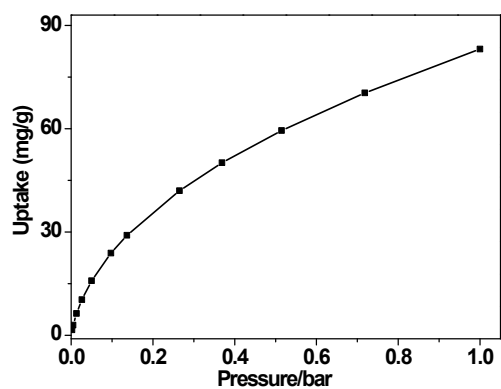


Figure S14. CO₂ sorption isotherm for Ag@3D-HNU5 at 273K.

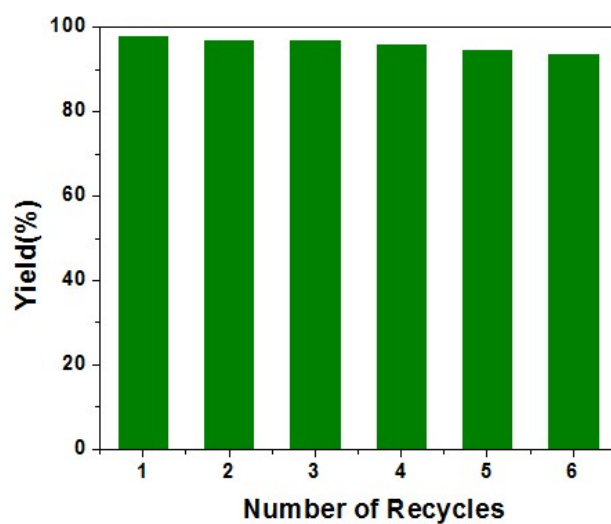


Figure S15. Recycle test of the 3D-HNU5@Ag in the cycloaddition reaction of CO₂ and propargylic alcohol to form cyclic carbonate.

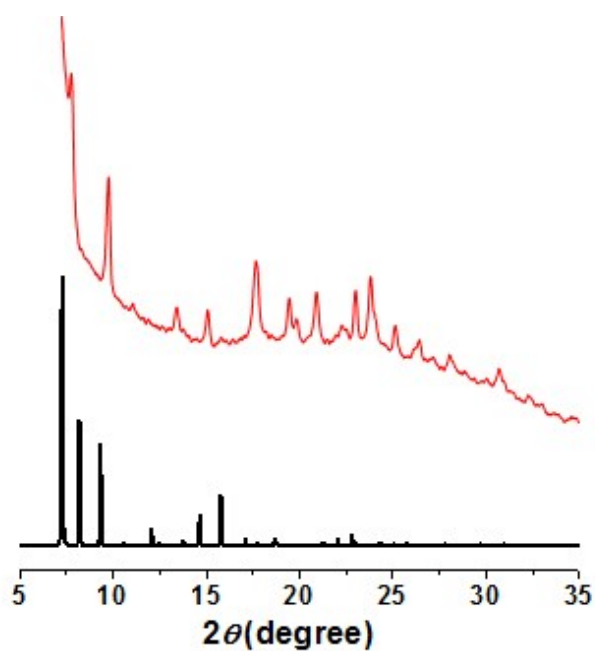


Figure S16. PXRD patterns of the 3D-HNU5 after 6 catalytic cycles.

Section S3: Tables

Table S1. Unit cell parameters and fractional atomic coordinates for 3D-HNU5 based on the two-interpenetrated diamond net

Space group	<i>P</i> 42/N (No.86)		
Unit cell	a= b=15.143488Å c= 19.967805 Å $\alpha=\beta=\gamma=90^\circ$		
C1	-0.68169	-0.37780	-0.35626
C2	-0.59646	-0.34397	-0.36623
C3	-0.53958	-0.38319	-0.41256
C4	-0.56693	-0.45578	-0.45186
C5	-0.65147	-0.49160	-0.43900
C6	-0.70830	-0.45228	-0.39261
H1	-0.57341	-0.28754	-0.33787
H2	-0.47363	-0.35653	-0.41810
H3	-0.67379	-0.55129	-0.46334
H4	-0.77298	-0.48091	-0.38450
N1	-0.72059	-0.26880	-0.27298
C7	-0.74308	-0.33756	-0.30756
H5	-0.80814	-0.36606	-0.30075
C8	-0.50000	-0.50000	-0.50000

Table S2. Unit cell parameters and fractional atomic coordinates for 3D-HNU5 based on the non-interpenetrated diamond net

Space group	<i>I</i> 41/ <i>A</i> (No.88)		
Unit cell	a=b=21.416126Å c=19.393561Å $\alpha=\beta=\gamma=90^\circ$		
C1	0.52975	1.15194	0.17813
C2	0.47021	1.12625	0.18312
C3	0.46139	1.07820	0.20628
C4	0.51136	1.05558	0.22593
C5	0.57153	1.07994	0.21950
C6	0.58029	1.12801	0.19630
H1	0.43047	1.14294	0.16894
H2	0.41508	1.05855	0.20905
H3	0.61254	1.06125	0.23167
H4	0.62695	1.14604	0.19225
N1	0.49470	1.22590	0.13649
C7	0.54032	1.20276	0.15378
H5	0.58710	1.22104	0.15037
C8	0.50000	1.00000	0.25000

Table S3. Unit cell parameters and fractional atomic coordinates for 3D-HNU5 based on the three-interpenetrated diamond net

Space group	<i>I</i> 41/ <i>A</i> (No.88)		
Unit cell	a= b=21.416126Å c=13.31187 Å $\alpha=\beta=\gamma=90^\circ$		
C1	0.52975	0.65194	0.78439
C2	0.47021	0.62625	0.79935
C3	0.46139	0.57820	0.86883
C4	0.51136	0.55558	0.92780
C5	0.57153	0.57994	0.90849
C6	0.58029	0.62801	0.83891
H1	0.43047	0.64294	0.75681
H2	0.41508	0.55855	0.87715
H3	0.61254	0.56125	0.94501
H4	0.62695	0.64604	0.82675
N1	0.49470	0.72590	0.65948
C7	0.54032	0.70276	0.71134
H5	0.58710	0.72104	0.70112
C8	0.50000	0.50000	1.00000

Table S4. Unit cell parameters and fractional atomic coordinates for 3D-HNU5 based on the four-interpenetrated diamond net

Space group	<i>P4</i> /N (No.85)		
Unit cell	a= b=15.143488 Å c=9.983902 Å $\alpha=\beta=\gamma=90^\circ$		
C1	0.68169	-0.37780	0.71252
C2	0.59646	-0.34397	0.73247
C3	0.53958	-0.38319	0.82511
C4	0.56693	-0.45578	0.90373
C5	0.65147	-0.49160	0.87799
C6	0.70830	-0.45228	0.78522
H1	0.57341	-0.28754	0.67575
H2	0.47363	-0.35653	0.83620
H3	0.67379	-0.55129	0.92668
H4	0.77298	-0.48091	0.76900
N1	0.72059	-0.26880	0.54597
C7	0.74308	-0.33756	0.61513
H5	0.80814	-0.36606	0.60150
C8	0.50000	-0.50000	1.00000

Table S5. Unit cell parameters and fractional atomic coordinates for 3D-HNU5 based on the five-interpenetrated diamond net

Space group	<i>I4</i> 1/A(No.88)		
Unit cell	a= b=21.416126Å c= 7.987122 Å $\alpha=\beta=\gamma=90^\circ$		
C1	0.52975	0.15194	0.89065
C2	0.47021	0.12625	0.91559
C3	0.46139	0.07820	1.03139
C4	0.51136	0.05558	1.12966
C5	0.57153	0.07994	1.09749
C6	0.58029	0.12801	0.98152
H1	0.43047	0.14294	0.84469
H2	0.41508	0.05855	1.04525
H3	0.61254	0.06125	1.15835
H4	0.62695	0.14604	0.96125
N1	0.49470	0.22590	0.68246
C7	0.54032	0.20276	0.76891
H5	0.58710	0.22104	0.75187
C8	0.50000	0.00000	1.25000

Table S6. Porosity parameters and CO₂ capture capacity at 273K for 3D-HNU5 and the selected 3D non-interpenetrated COFs

COF	Covalent bond type	SA _{BET} [m ² g ⁻¹]	Pore width [nm]	low-pressure CO ₂ capacity [mg/g]	Ref.
CD-COF- Li (non-interpenetrated)	boronate	760	0.5-1	130	<i>Angew. Chem. Int. Ed.</i> 2017, 56, 16313.
CD-COF- DMA (non-interpenetrated)	boronate	934	0.5-1.5	128	<i>Angew. Chem. Int. Ed.</i> 2017, 56, 16313.
CD-COF- PPZ (non-interpenetrated)	boronate	494	0.5-1	130	<i>Angew. Chem. Int. Ed.</i> 2017, 56, 16313.
DL-COF-1 (non-interpenetrated)	boroxine and imine	2259	1.4	272	<i>J. Am. Chem. Soc.</i> 2016, 138, 14783.
DL-COF-1 (non-interpenetrated)	boroxine and imine	2071	1.3	222	<i>J. Am. Chem. Soc.</i> 2016, 138, 14783
COF-102 (non-interpenetrated)	boroxine	2497	1.2	66.8	<i>J. CO₂ Utili.</i> 2017, 17, 137
COF-103 (non-interpenetrated)	Boronate	3620	1.3	74.6	<i>J. CO₂ Utili.</i> 2017, 17, 137
3D-Py-COF (interpenetrated)	imine	1290	0.59	156	<i>J. Am. Chem. Soc.</i> 2016, 138, 3302.
3D-ionic-COFs-1 (interpenetrated)	imine	966	0.86	161	<i>J. Am. Chem. Soc.</i> 2017, 139, 17771.
3D-ionic-COFs-2 (interpenetrated)	imine	880	0.82	133	<i>J. Am. Chem. Soc.</i> 2017, 139, 17771.
3D- COF-1a (interpenetrated)	imine	596	0.83	45 ^a	<i>J. Am. Chem. Soc.</i> 2018, 140, 4494.
3D- IL-COF-1 (interpenetrated)	imine	517	0.83	53 ^a	<i>J. Am. Chem. Soc.</i> 2018, 140, 4494.
3D- IL-COF-2 (interpenetrated)	imine	653	1.07	76 ^a	<i>J. Am. Chem. Soc.</i> 2018, 140, 4494.
3D- IL-COF-3 (interpenetrated)	imine	870	1.24	49 ^a	<i>J. Am. Chem. Soc.</i> 2018, 140, 4494.
3D-HNU5	azine	864	1.0	123	This work

^a The CO₂ uptakes were measured at 298K.

